Optical Coherence Tomography Velocimetry of Colloidal Suspensions-

Supplementary Information

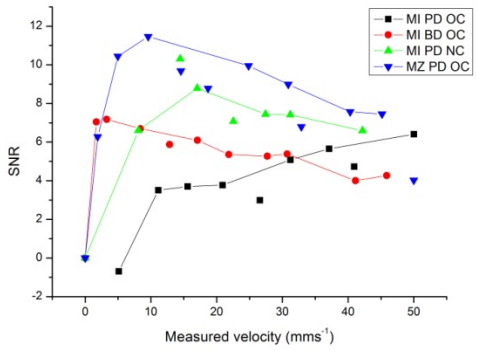

Figure 1: Comparison of measured signal to noise as a function of shear velocity ($\propto \omega$) for different embodiments of the OCT Velocimetry device. This shows that the original setup, (black squares) suffered greatly from the effects of *1/f* noise as the SNR deteriorates for low velocities. Increasing the sampling frequency (green triangles) improves SNR however it is still low for low velocities. Balanced detection (red circles) improves SNR at low velocities by removing common noise within the system, and the use of a Mach Zender interferometer with modulation techniques increases the SNR for all velocities (blue triangles). Whilst these curves decrease at higher velocities as a consequence of the noise equivalent bandwidth (NEB) increasing with beat frequency, this plot clearly shows that SNR is significantly increased by these changes to the setup.

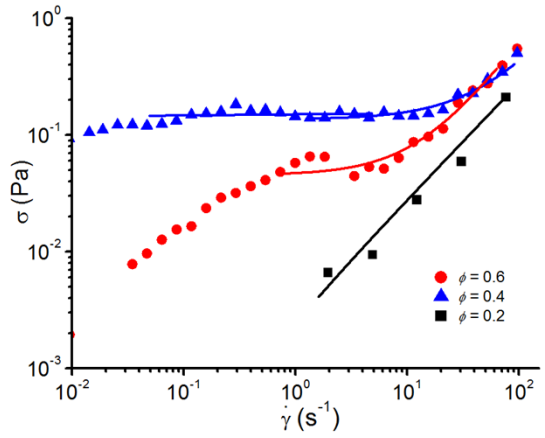

Figure 2: Enlargement of the inset from Figure 3: Measured stress (σ) as a function of shear rate for different volume fractions of polystyrene colloid suspensions, displaying Herschel-Buckley type behaviour (fits shown on the figure) for $\phi = 0.4$ and $\phi = 0.6$ volume fraction suspensions according to Equation 2. The ϕ= 0.2 suspensions follow linear fits.

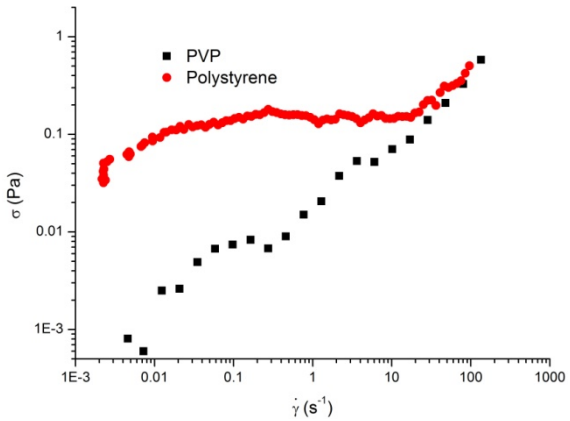

Figure 3: Bulk rheology for $\phi = 0.4$ suspensions of PVP and Polystyrene colloids, showing that at low enough shear rates the sample behaves as a fluid and the stress approaches zero.

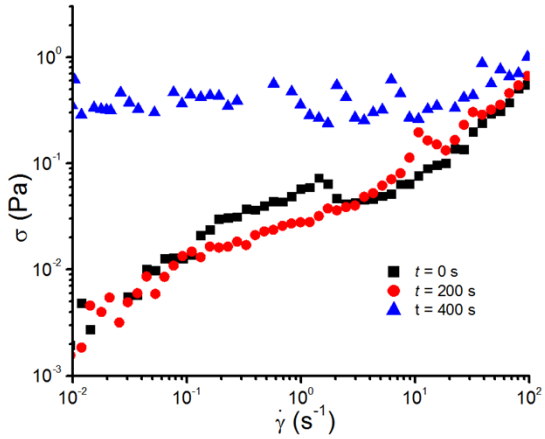

Figure 4: Enlargement of the inset from Figure 4: Stress as a function of shear rate for a $\phi = 0.6$ suspension of thixotropic polystyrene colloids over time. The legend gives the time elapsed after loading the sample when the shear ramp experiment began.

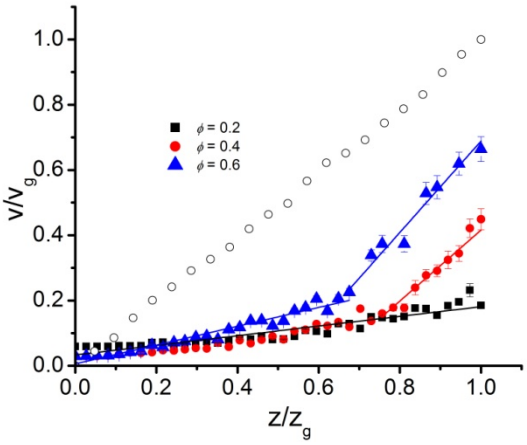

Figure 5: Enlargement of the inset from Figure 5: Rescaled shear velocity (v/v_g) as a function of rescaled depth across the rheometer gap (z/z_g) for three different volume fraction suspensions of polystyrene colloids (γ = 50 s^{-1}). The open circles show the profile for a dilute suspenion of silica tracer paticles used to calibrate the experiment. The error bars signify the apparent velocity fluctuations at each depth within the sample.

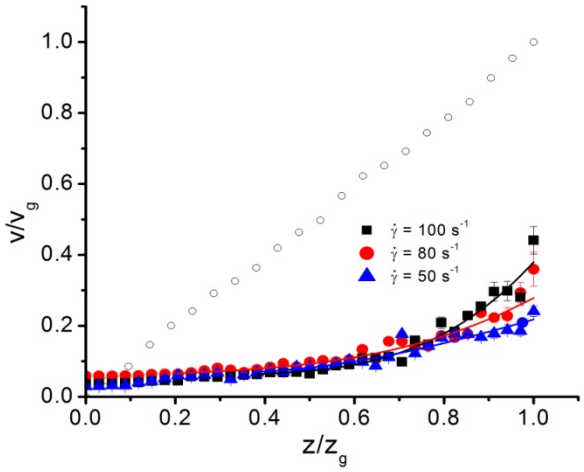

Figure 6: Enlargement of the inset from Figure 6: Scaled shear velocity (v/v_g) as a function of normalized distance across the rheometer gap (z/z_g) for dense suspensions of polystyrene hard spheres (ϕ = 0.6), showing shear banding and slipping at the upper plate (z/z_g = 1). The error bars signify the apparent velocity fluctuations at each depth within the sample. The open circles show the profile for a dilute suspension of silica tracer particles.

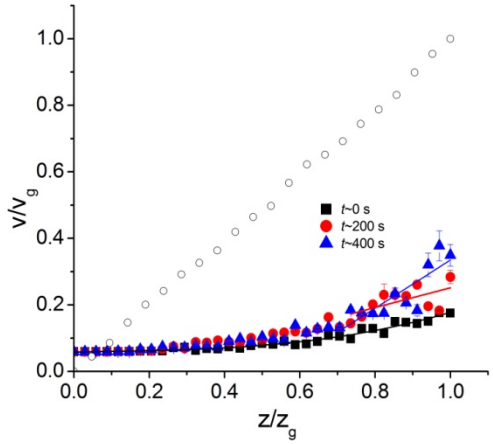

Figure 7: Enlargement of the inset from Figure 7: Shear velocity as a function of depth across the rheometer gap for a ϕ = 0.6 polystyrene suspensions with steady shear rate of 50 s^{-1} recorded at different intervals after sample loading. Thixotropy of the samples is evident in the velocity profiles. The open circles show the profile for a dilute suspension of silica tracer particles.

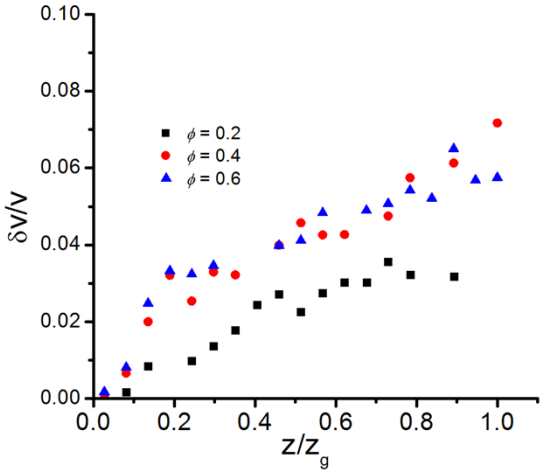

Figure 8: Enlargement of the inset from Figure 8: Reduced velocity fluctuations ($\delta v/v$) as a function of distance (z/z_g) across the rheometer gap for dense polystyrene suspensions (ϕ = 0.6).